

## Structure of amplitudes of $KN$ charge-exchange reactions

E. N. Argyres\*

*State University College of Arts and Science, Plattsburgh, New York 12901*

A. P. Contogouris and J. P. Holden†

*Department of Physics, McGill University, Montreal, Canada*

(Received 20 May 1974)

On the basis of recent data on  $K^-p \rightarrow \bar{K}^0n$  polarization and on differential cross sections, we present an amplitude analysis for  $K^-p \rightarrow \bar{K}^0n$  and  $K^+n \rightarrow K^0p$ . The approach makes use of fixed- $t$  dispersion relations and of information in the low-energy (resonance) region. We present detailed comparison of our results with those of amplitude analyses of other reactions, and we underline a number of features of the vector and tensor exchange in common to several two-body hadron processes. A check of our results against finite-energy sum rules is also presented.

### I. INTRODUCTION

The structure of the real and imaginary parts of the amplitudes as functions of the momentum transfer  $\sqrt{-t}$  has been one of the most important preoccupations of two-body phenomenology in the past few years.<sup>1-8</sup> A main purpose of this effort is to determine those specific features which are the same in a number of hadron reactions and which may eventually lead to a satisfactory theory of two-body processes.

Recently the polarization for  $K^-p \rightarrow \bar{K}^0n$  has been measured at 8 GeV.<sup>9</sup> The purpose of this work is to combine this measurement with data on differential cross sections of  $K^-p \rightarrow \bar{K}^0n$  and  $K^+n \rightarrow K^0p$  in order to obtain what amounts to an amplitude analysis for these two reactions. The approach makes use of fixed- $t$  dispersion relations (DR) and of information in the low-energy (resonance) region of  $KN$  charge exchange (CEX). With certain variations the same approach has been applied to a number of two-body processes with very satisfactory results.<sup>10-15,5,8</sup>

At high energy the reactions  $K^-p \rightarrow \bar{K}^0n$  and  $K^+n \rightarrow K^0p$  are determined in terms of a vector  $t$ -channel exchange with the quantum numbers of the  $\rho$  meson and of a tensor exchange with those of  $A_2$ . We determine the real and imaginary parts of the  $s$ -channel helicity amplitudes for these two exchanges at 8 GeV. Our results are compared in detail with those of other amplitude analyses involving vector and tensor exchanges, and a number of common specific features are pointed out. In particular, a rather definite form of the real part of the nonflip amplitude for both vector and tensor exchange seems to emerge [Sec. III points (vi) and (vii)]; this is hoped to be useful towards eventually forming a satisfactory model for this amplitude.

Section II presents our dispersion formalism. Section III discusses the details of our approach, presents our amplitude analysis, compares it with analyses of other reactions, and underlines a number of common features. Section IV checks our results against finite-energy sum rules (FESR) and also compares them with the results of certain very recent analyses of  $KN$  CEX.

### II. FORMALISM

We will describe here the basic formalism used to discuss the two line-reversed reactions shown in Fig. 1.<sup>16</sup> The  $s$  channel is taken as  $K^+n \rightarrow K^0p$  and is described by the usual invariant amplitudes  $A(\nu, t)$ ,  $B(\nu, t)$ , where  $4M = s - u$  and  $M$  is the nucleon mass. The corresponding  $u$ -channel amplitudes describing  $K^-p \rightarrow \bar{K}^0n$  are denoted by  $\bar{A}(\nu, t)$  and  $\bar{B}(\nu, t)$ . We form crossing-even (-odd) forms corresponding to  $A_2(\rho)$  exchanges by taking sums (differences)

$$A^{(\pm)}(\nu, t) = \frac{1}{2}[A(\nu, t) + \bar{A}(\nu, t)], \quad (2.1)$$

and similarly for  $B^{(\pm)}$ . The corresponding nonflip and flip  $s$ -channel helicity amplitudes  $F_n(\nu, t)$  are given to leading order in  $\nu$  by

$$F_0^{(\pm)}(\nu, t) = -2M[A^{(\pm)}(\nu, t) \pm \nu B^{(\pm)}(\nu, t)], \quad (2.2)$$

$$F_1^{(\pm)}(\nu, t) = -\sqrt{-t} A^{(\pm)}(\nu, t). \quad (2.3)$$

The amplitudes for  $K^+n \rightarrow K^0p$  are then  $F_n = F_n^{(+)} + F_n^{(-)}$ , while those for  $K^-p \rightarrow \bar{K}^0n$  are  $\bar{F}_n = F_n^{(+)} - F_n^{(-)}$  ( $n=0, 1$ ). With these conventions exchange degeneracy for the vector and tensor exchanges implies  $\text{Im}F_n^{(+)} = -\text{Im}F_n^{(-)}$ . The amplitudes are so normalized that the differential cross section and polarization in the  $s$  channel are given by

$$\frac{d\sigma}{dt} = \frac{1}{16\pi s^2} (|F_0|^2 + |F_1|^2), \quad (2.4)$$

$$p \frac{d\sigma}{dt} = \frac{1}{8\pi s^2} \text{Im}(F_0 F_1^*). \quad (2.5)$$

Analogous relations hold for the barred ( $u$  channel) amplitudes.

The real parts of the invariant amplitudes will be calculated from the imaginary parts by means of the DR<sup>17</sup>

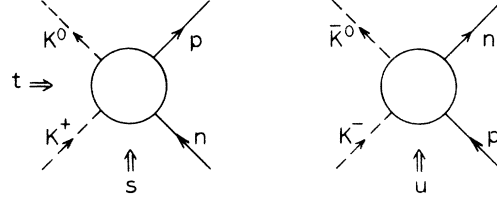


FIG. 1. Kinematics of the  $KN$  CEX reactions.

$$\begin{aligned} \text{Re}A_p^\pm(\nu, t) = & -\frac{1}{2M} \frac{g_\Lambda^2(M_\Lambda - M)}{\nu_\Lambda \pm \nu} - \frac{1}{2M} \frac{g_\Sigma^2(M_\Sigma - M)}{\nu_\Sigma \pm \nu} + \frac{1}{\pi} \int_{\nu_0}^{\infty} d\nu' \frac{\text{Im}A_p^+(\nu', t)}{\nu' \mp \nu} \\ & + \frac{1}{\pi} \int_{\nu_0}^{\infty} d\nu' \frac{\text{Im}A_p^-(\nu', t)}{\nu' \pm \nu} + \frac{1}{\pi} \int_{\bar{\nu}}^{\nu_0} d\nu' \frac{\text{Im}A_p^-(\nu', t)}{\nu' \pm \nu}, \end{aligned} \quad (2.6)$$

$$\text{Re}B_p^\pm(\nu, t) = \mp \frac{1}{2M} \mp \frac{g_\Sigma^2}{\nu_\Sigma \pm \nu} \pm \frac{1}{\pi} \int_{\nu_0}^{\infty} d\nu' \frac{\text{Im}B_p^+(\nu', t)}{\nu' \mp \nu} \mp \int_{\nu_0}^{\infty} d\nu' \frac{\text{Im}B_p^-(\nu', t)}{\nu' \pm \nu} \mp \frac{1}{\pi} \int_{\bar{\nu}}^{\nu_0} d\nu' \frac{\text{Im}B_p^-(\nu', t)}{\nu' \pm \nu}, \quad (2.7)$$

where  $A_p^\pm, B_p^\pm$  are the invariant amplitudes for  $K^+p$  elastic scattering. Analogous relations hold for  $A_n^\pm, B_n^\pm$ , the invariant amplitudes for  $K^+n$  elastic scattering, with the subscript  $p$  replaced by  $n$  everywhere in Eqs. (6) and (7),  $g_\Lambda^2$  replaced by zero and  $g_\Sigma^2$  by  $2g_\Sigma^2$ . In these equations  $g_\Lambda$  and  $g_\Sigma$  are the couplings of  $\Lambda(1.115, \frac{1}{2}^+)$  and  $\Sigma(1.194, \frac{1}{2}^+)$  to the  $KN$  system,  $\nu_\Lambda, \nu_\Sigma$  are the values of  $\nu$  corresponding to  $s = M_\Lambda^2$  and  $s = M_\Sigma^2$ ,  $\nu_0$  corresponds to the  $KN$  threshold and  $\bar{\nu}$  to the  $\pi\Lambda$  threshold. Since the  $\pi\Lambda$  decay channel is open at the threshold of the  $\bar{K}N$  system, Eqs. (6) and (7) contain extra integrals over the unphysical region  $\bar{\nu} \leq \nu \leq \nu_0$ ; also, since there is no physical state with strangeness +1 and  $(\text{mass})^2 < (M_K + M_N)^2$ ,  $\text{Im}A_{p(n)}^+ = \text{Im}B_{p(n)}^+ = 0$  in this region.

To obtain DR for  $A^{(\pm)}, B^{(\pm)}$  we use isotopic spin invariance, which says

$$A = A_p^+ - A_n^+, \quad \bar{A} = A_p^- - A_n^-,$$

and thus through Eq. (1)

$$A^{(\pm)} = \frac{1}{2}(A_p^\pm \pm A_n^\pm - A_n^\mp \mp A_p^\mp), \quad (2.8)$$

and analogously for  $B$ .

Following a procedure that has led to satisfactory results in several other two-body reactions, we split the dispersion integrals into two pieces: a low-energy piece ( $\nu < N$ , to be specified later) and a high-energy piece ( $\nu > N$ ).

In the high-energy piece the imaginary parts of the amplitudes are taken to be the effective Regge forms

$$\begin{aligned} \text{Im}A^{(\pm)}(\nu, t) & \simeq \text{Im}A_{\text{asy}}^{(\pm)}(\nu, t) \\ & = a^{(\pm)}(t) \left\{ \begin{matrix} (\nu^2 - \nu_0^2)^{\nu/2} \\ \nu \end{matrix} \right\} \\ & \quad \times (\nu^2 - \nu_0^2)^{[\alpha_+(t)-1]/2}, \end{aligned} \quad (2.9)$$

$$\begin{aligned} \text{Im}B^{(\pm)}(\nu, t) & \simeq \text{Im}B_{\text{asy}}^{(\pm)}(\nu, t) \\ & = b^{(\pm)}(t) \left\{ \begin{matrix} \nu \\ (\nu^2 - \nu_0^2)^{1/2} \end{matrix} \right\} \\ & \quad \times (\nu^2 - \nu_0^2)^{[\alpha'_\pm(t)-1]/2}, \end{aligned} \quad (2.10)$$

where in the curly brackets the upper (lower) function of  $\nu$  corresponds to the crossing-even (-odd) amplitude and  $\alpha_\pm(t), \alpha'_\pm(t)$  are effective Regge poles. Specifically  $\text{Im}A_{\text{asy}}^{(-)}, \text{Im}B_{\text{asy}}^{(-)}$  represent the effective vector ( $\rho$ ) contribution, while  $\text{Im}A_{\text{asy}}^{(+)}, \text{Im}B_{\text{asy}}^{(+)}$  represent the effective tensor ( $A_2$ ) contribution. The two trajectories need not be the same; however, for simplicity we shall assume

$$\begin{aligned} \alpha'_+(t) & = \alpha_+(t) = \alpha_{A_2}(t), \\ \alpha'_-(t) & = \alpha_-(t) = \alpha_\rho(t) \end{aligned}$$

and in fact that

$$\alpha_{A_2}(t) = \alpha_\rho(t) \equiv \alpha(t) = 0.45 + 0.9t. \quad (2.11)$$

As for the low-energy pieces ( $\nu < N$ ), since there are no well-established resonances of hypercharge  $Y=2$  and since the general amplitude  $M$  for  $K^+n \rightarrow K^0p$  satisfies

$$M(K^+n \rightarrow K^0p) = \frac{1}{2}(M_{Y=2}^{IS=1} - M_{Y=2}^{IS=0}),$$

we have

$$\text{Im}A(\nu, t) = \text{Im}B(\nu, t) = 0 \quad (\nu \leq N).$$

Via Eq. (1) this implies

$$\begin{aligned} \text{Im}A^{(+)}(\nu, t) &= -\text{Im}A^{(-)}(\nu, t) \\ &= \text{Im}\bar{A}(\nu, t), \\ \text{Im}B^{(+)}(\nu, t) &= -\text{Im}B^{(-)}(\nu, t) \\ &= \text{Im}\bar{B}(\nu, t) \quad (\nu \leq N). \end{aligned} \quad (2.12)$$

Also, since the general amplitude  $\bar{M}$  for  $K^-p \rightarrow K^0n$  satisfies

$$\begin{aligned} \bar{M}(K^-p \rightarrow K^0n) &= -\frac{1}{2}(M_{Y=0}^{I_S=1} - M_{Y=0}^{I_S=0}) \\ &= -\frac{1}{2}(M_{\Sigma^*} - M_{\Lambda^*}), \end{aligned}$$

we have

$$\begin{aligned} \text{Im}\bar{A}(\nu, t) &= -\frac{1}{2}(\text{Im}\bar{A}_{\Sigma^*} - \text{Im}\bar{A}_{\Lambda^*}), \\ \text{Im}\bar{B}(\nu, t) &= -\frac{1}{2}(\text{Im}\bar{B}_{\Sigma^*} - \text{Im}\bar{B}_{\Lambda^*}) \quad (\nu \leq N). \end{aligned} \quad (2.13)$$

Before we present the final form of our DR we note that, in view of (2.9) and of its crossing-even property, the amplitude  $A^{(+)}(\nu, t)$  requires one subtraction. We define

$$\begin{aligned} \text{Re}A_{\text{asy}}^{(+)} &= \text{Im}A_{\text{asy}}^{(+)} \left\{ \begin{array}{l} -\cot\frac{1}{2}\pi\alpha \\ \tan\frac{1}{2}\pi\alpha \end{array} \right\}, \\ \text{Re}B_{\text{asy}}^{(+)} &= \text{Im}B_{\text{asy}}^{(+)} \left\{ \begin{array}{l} -\cot\frac{1}{2}\pi\alpha \\ \tan\frac{1}{2}\pi\alpha \end{array} \right\}, \end{aligned} \quad (2.14)$$

and we proceed by writing a DR for the difference  $A^{(+)} - A_{\text{asy}}^{(+)}$ . The rest of the amplitudes do not require subtractions; however, we can write all DR in common form by applying well-known Hilbert transforms to the high-energy piece ( $\nu > N$ ) of the dispersion integrals (for more details see the Appendix of Ref. 12).

Then with (2.8), (2.12), and (2.13) the DR (2.6) and (2.7) become

$$\begin{aligned} \text{Re}A^{(+)}(\nu, t) &= \frac{g_{\Sigma}^2(M_{\Sigma} - M)}{4M} \left( \frac{1}{\nu_{\Sigma} + \nu} \pm \frac{1}{\nu_{\Sigma} - \nu} \right) - \frac{g_{\Lambda}^2(M_{\Lambda} - M)}{4M} \left( \frac{1}{\nu_{\Lambda} + \nu} \pm \frac{1}{\nu_{\Lambda} - \nu} \right) + \text{Re}A_{\text{asy}}^{(+)}(\nu, t) \\ &\quad + \frac{1}{\pi} \int_{\nu}^{\nu_0} d\nu' \text{Im}\bar{A}(\nu', t) \left( \frac{1}{\nu' + \nu} \pm \frac{1}{\nu' - \nu} \right) + \frac{1}{\pi} \int_{\nu_0}^N d\nu' \text{Im}A^{(+)}(\nu', t) \left( \frac{1}{\nu' + \nu} \pm \frac{1}{\nu' - \nu} \right) \\ &\quad - a^{(+)}(t) \left\{ \begin{array}{l} 1 \\ \nu \end{array} \right\} S^{(+)}(\alpha, \nu), \end{aligned} \quad (2.15)$$

$$\begin{aligned} \text{Re}B^{(+)}(\nu, t) &= \frac{g_{\Sigma}^2}{4M} \left( \frac{1}{\nu_{\Sigma} + \nu} \mp \frac{1}{\nu_{\Sigma} - \nu} \right) - \frac{g_{\Lambda}^2}{4M} \left( \frac{1}{\nu_{\Lambda} + \nu} \mp \frac{1}{\nu_{\Lambda} - \nu} \right) + \text{Re}B_{\text{asy}}^{(+)}(\nu, t) \\ &\quad - \frac{1}{\pi} \int_{\nu}^{\nu_0} d\nu' \text{Im}\bar{B}(\nu', t) \left( \frac{1}{\nu' + \nu} \mp \frac{1}{\nu' - \nu} \right) - \frac{1}{\pi} \int_{\nu_0}^N d\nu' \text{Im}B^{(+)}(\nu', t) \left( \frac{1}{\nu' + \nu} \mp \frac{1}{\nu' - \nu} \right) \\ &\quad - b^{(+)}(t) \left\{ \begin{array}{l} \nu \\ 1 \end{array} \right\} S^{(+)}(\alpha - 1, \nu), \end{aligned} \quad (2.16)$$

where

$$\begin{aligned} S^{(+)}(\alpha, \nu) &= \frac{1}{\pi} \int_{\nu_0}^N d\nu' \frac{2\nu'(\nu'^2 - \nu_0^2)^{\alpha/2}}{\nu'^2 - \nu^2} \\ &= -\sum_{n=0}^{\infty} (n + 1 + \frac{1}{2}\alpha)^{-1} \left( \frac{N^2 - \nu_0^2}{\nu^2 - \nu_0^2} \right)^{n+1+\alpha/2}. \end{aligned}$$

In the calculation of the integrals of (2.15), (2.16) we use the relations (2.12) and (2.13) for the imaginary parts; these, in turn, are evaluated by resonance saturation; then  $N$  corresponds to the mass of the highest resonance to be included (Sec. III).

By expanding  $1/(\nu' + \nu)$  in the integrands of (2.15) and (2.16) in powers of  $1/\nu$ , we easily obtain the following FESR:

$$-\pi\nu_{\Lambda} \frac{g_{\Lambda}^2(M_{\Lambda} - M)}{4M} + \pi\nu_{\Sigma} \frac{g_{\Sigma}^2(M_{\Sigma} - M)}{4M} + \int_{\nu}^{\nu_0} d\nu \nu \text{Im}\bar{A}(\nu, t) + \int_{\nu_0}^N d\nu \nu \text{Im}A^{(+)}(\nu, t) = \frac{a^{(+)}(t)(N^2 - \nu_0^2)^{[\alpha(t)+2]/2}}{\alpha(t) + 2}, \quad (2.17)$$

$$\pi \frac{g_{\Lambda}^2(M_{\Lambda} - M)}{4M} - \pi \frac{g_{\Sigma}^2(M_{\Sigma} - M)}{4M} - \int_{\nu}^{\nu_0} d\nu \text{Im}\bar{A}(\nu, t) + \int_{\nu_0}^N d\nu \text{Im}A^{(-)}(\nu, t) = \frac{a^{(-)}(t)(N^2 - \nu_0^2)^{[\alpha(t)+1]/2}}{\alpha(t) + 1}, \quad (2.18)$$

$$\pi \frac{g_{\Lambda}^2}{4M} - \frac{\pi g_{\Sigma}^2}{4M} + \int_{\bar{\nu}}^{\nu_0} d\nu \text{Im}\bar{B}(\nu, t) + \int_{\nu_0}^N d\nu \text{Im}B^{(+)}(\nu, t) = \frac{b^{(+)}(t)(N^2 - \nu_0^2)^{\alpha(t)/2}}{\alpha(t)}, \quad (2.19)$$

$$-\pi \nu_{\Lambda} \frac{g_{\Lambda}^2}{4M} + \pi \nu_{\Sigma} \frac{g_{\Sigma}^2}{4M} - \int_{\bar{\nu}}^{\nu_0} d\nu \nu \text{Im}\bar{B}(\nu, t) + \int_{\nu_0}^N d\nu \nu \text{Im}B^{(-)}(\nu, t) = \frac{b^{(-)}(t)(N^2 - \nu_0^2)^{[\alpha(t)+1]/2}}{\alpha(t)+1}. \quad (2.10)$$

We shall make use (Sec. IV) of the lowest-moment FESR.

### III. PROCEDURE: RESULTING AMPLITUDES AND THEIR MAIN FEATURES

At each value of  $t$  the formalism of Sec. II contains four parameters:  $a^{(+)}(t)$  and  $b^{(+)}(t)$ . In principle, these can be determined from experimental data on the differential cross sections  $d\sigma/dt$  and on the polarizations  $P$  for  $K^-p \rightarrow \bar{K}^0n$  and  $K^+n \rightarrow K^0p$  at one energy. Unfortunately, data on  $P(K^+n \rightarrow K^0p)$  are not available at present. We thus assume that the imaginary parts of our flip amplitudes for the effective  $\rho$  and  $A_2$  contribution are exchange-degenerate (EXD), i.e., that the relation (2.11),

$$\text{Im}A^{(+)}(\nu, t) = -\text{Im}A^{(-)}(\nu, t), \quad (3.1)$$

holds also for  $\nu > N$ . Exchange degeneracy for the flip amplitudes (although not necessarily in strong form) is consistent with the  $d\sigma/dt$  data above 5 GeV [Figs. 3 and 4 (see Refs. 31–33)], with the relative magnitude and  $t$  structure of the polarizations for  $K^+p$  elastic scattering,<sup>18</sup> and with several phenomenological analyses.<sup>19</sup> At sufficiently high  $\nu$  ( $\gg \nu_0$ ) Eqs. (2.9) and (3.1) imply

$$a^{(+)}(t) = -a^{(-)}(t), \quad (3.2)$$

so that we need as input only three pieces of experimental information. We shall use the polarization data for  $K^-p \rightarrow \bar{K}^0n$  at 8 GeV (Fig. 2, solid line), and the differential cross sections for  $K^-p \rightarrow \bar{K}^0n$  at 12.3 GeV (Fig. 3) and for  $K^+n \rightarrow K^0p$  at 12 GeV (Fig. 4).

The best way to calculate the low-energy integrals of (2.15) and (2.16) would be in terms of partial-wave phase-shift analyses. However, the available analyses are incomplete and cover only very low energies; thus we proceed by saturating the low-energy imaginary parts by the known  $\bar{K}N$  resonances. In fact we use the narrow-resonance approximation, which has already led to satisfactory results.<sup>20</sup> Then a resonance of spin  $J$ , mass  $M_J$ , width  $\Gamma_J$ , and elasticity  $x_{\bar{K}N}$  contributes to the imaginary part of the partial wave  $f_{(J+1/2)^{\mp}}(s)$  a term

$$\text{Im}f_{(J+1/2)^{\mp}}(s) = \frac{\pi x_{\bar{K}N} M_J \Gamma_J}{q} \delta(S - M_J^2), \quad (3.3)$$

where  $q$  is the c.m. momentum. Well-known partial-wave expansions are then used to calculate  $\text{Im}\bar{A}, \text{Im}\bar{B}$ . The integrals over the unphysical region  $\bar{\nu} \leq \nu \leq \nu_0$  are saturated by the  $\Lambda'(1405)$  and  $\Sigma'(1385)$  resonances, which are below the  $\bar{K}N$  threshold; for the explicit contributions of these resonances to  $\text{Im}\bar{A}, \text{Im}\bar{B}$ , see Ref. 20. The resonance parameters (widths  $\Gamma_J$  and elasticities  $x_{\bar{K}N}$ ) used throughout the work are shown in Table I, and correspond to mean values of Particle Data tables.<sup>21</sup> Also, Table I shows the couplings used for the  $\Lambda, \Lambda'$  and  $\Sigma, \Sigma'$  below threshold. For the  $KN\Lambda$  and  $KN\Sigma$  coupling constants we use values close to those of a number of authors<sup>20,22,23</sup>; and the couplings of the  $\Lambda'(1405)$  and  $\Sigma'(1385)$  have been chosen in accord with Ref. 24, which appears to provide one of the best determinations (see Ref. 22 and the second paper of Ref. 17).<sup>25</sup>

The real and imaginary parts of the resulting  $s$ -channel helicity amplitude at 8 GeV are shown in Fig. 5. Their essential features as well as certain implications and comparison with the re-

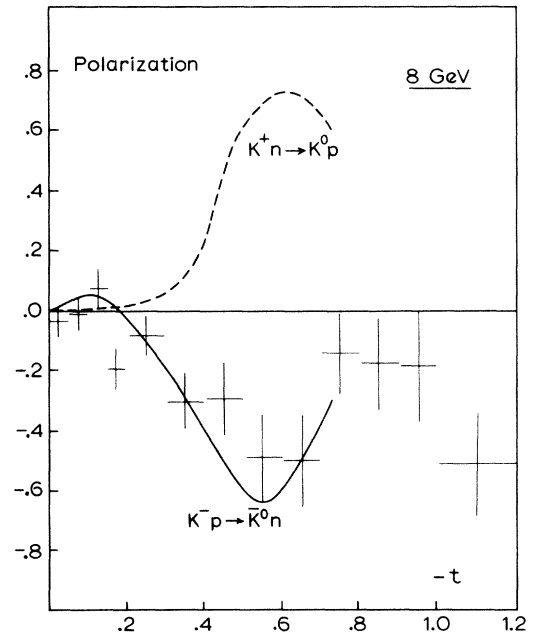


FIG. 2. Polarization of the  $KN$  CEX reactions at 8 GeV. Solid line: Input used in our amplitude analysis; data of Ref. 9. Broken line: Predicted polarization for  $K^+n \rightarrow K^0p$ .

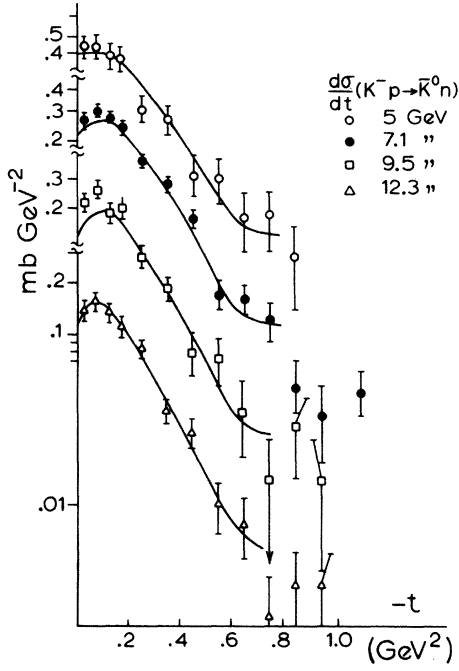


FIG. 3. Differential cross sections for  $K^-p \rightarrow \bar{K}^0n$ . The line through the data at 12.3 GeV has been used as input. The lines at 5, 7.1, and 9.5 GeV are predictions of our approach. Data from Ref. 31.

TABLE I. Resonance and pole parameters used in the calculation of the low-energy integrals. The widths are the mean values of Ref. 21.

Name $J^P$	$\Gamma$ (GeV)	$x_{\bar{K}N}$
$I=1, Y=0$		
$\Sigma'(1670) \frac{3}{2}^-$	0.05	0.08
$\Sigma''(1750) \frac{1}{2}^-$	0.075	0.15
$\Sigma(1765) \frac{5}{2}^-$	0.12	0.41
$\Sigma'(1910) \frac{5}{2}^+$	0.075	0.14
$\Sigma(2030) \frac{7}{2}^+$	0.135	0.20
$\Sigma(1194) \frac{1}{2}^+$	$g_{\Sigma KN^2}/4\pi = 1.13$	
$\Sigma'(1385) \frac{3}{2}^+$	$g_{\Sigma' KN^2}/4\pi = 0.21$	
$I=0, Y=0$		
$\Lambda'(1518) \frac{3}{2}^-$	0.016	0.45
$\Lambda''(1670) \frac{1}{2}^-$	0.026	0.20
$\Lambda''(1690) \frac{3}{2}^-$	0.056	0.25
$\Lambda'(1820) \frac{5}{2}^+$	0.084	0.61
$\Lambda'(1835) \frac{5}{2}^-$	0.105	0.10
$\Lambda'(2100) \frac{7}{2}^-$	0.10	0.25
$\Lambda(1115) \frac{1}{2}^+$	$g_{\Lambda KN^2}/4\pi = 14.2$	
$\Lambda'(1405) \frac{1}{2}^-$	$g_{\Lambda' KN^2}/4\pi = 0.32$	

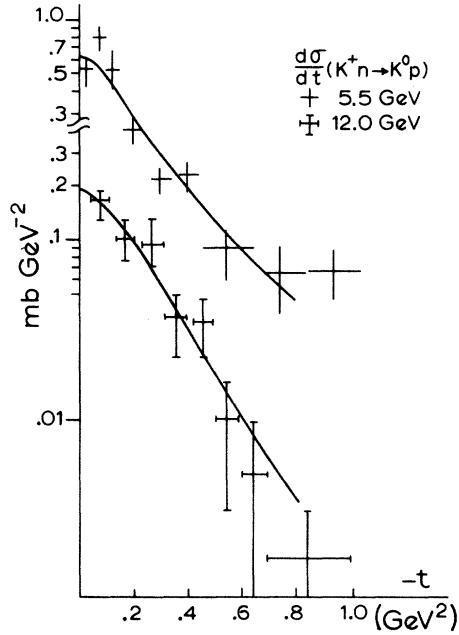


FIG. 4. Differential cross sections for  $K^+n \rightarrow K^0p$ . The line through the data at 12 GeV (Ref. 32) has been used as input. The line at 5.5 GeV is our prediction, and it is compared with data of Ref. 33.

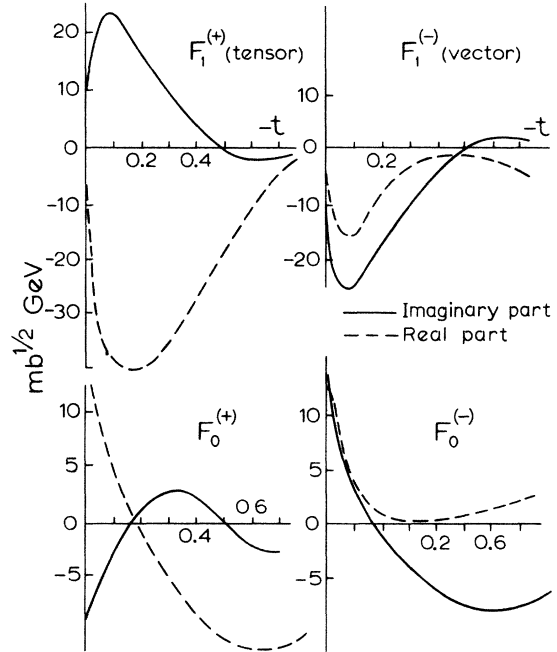


FIG. 5. The  $s$ -channel helicity amplitudes for the tensor ( $A_2$ ) and vector ( $\rho$ ) exchange in  $KN$  CEX at 8 GeV.

sults of other amplitude analyses are as follows:

(i) The imaginary parts of the flip amplitudes ( $\text{Im}F_1^{(\pm)}$ ) have a  $t$  structure in accord with the requirements of the dual absorptive model (DAM), namely  $\text{Im}F_1^{(\pm)} \sim J_1(R\sqrt{-t})$ , with  $R \approx 1$  F (hence  $\text{Im}F_1^{(\pm)}$  changes sign near  $t = -0.5$  GeV).

(ii) The real part of the flip amplitude for vector ( $\rho$ ) exchange ( $\text{Re}F_1^{(-)}$ ) satisfies approximately

$$\text{Re}F_1^{(-)} \approx \tan \frac{1}{2} \pi \alpha \text{Im}F_1^{(-)}, \quad (3.4)$$

where  $\alpha = \alpha(t)$  of Eq. (2.11). Together with (i), this relation results in a "double zero" structure of  $\text{Re}F_1^{(-)}$  near  $t = -0.5$ . This structure as well as (3.4) appear to be a common feature of most amplitude analyses<sup>3-8</sup> and should be considered as a well-established feature of vector exchange.

(iii) The real part of the flip amplitude for tensor ( $A_2$ ) exchange ( $\text{Re}F_1^{(+)}$ ) satisfies approximately

$$\text{Re}F_1^{(+)} \approx -\cot \frac{1}{2} \pi \alpha \text{Im}F_1^{(+)}.$$

This again appears as a common feature of several analyses involving tensor exchange.<sup>4-8</sup> Together with (i) and (ii), it implies that a good first approximation for  $F_1^{(\pm)}(\nu, t)$  is a single Regge-pole exchange [with a factor  $\alpha(t)$  in the residue]; absorption or secondary trajectories should make small corrections to the flip amplitudes. Notice the relatively large contribution of  $\text{Re}F_1^{(+)}$  at  $-t \approx 0.4-0.5$ ; this is known to be mainly responsible for the absence of dips near  $t \approx -0.5$  of the  $KN$  CEX cross sections.

(iv) The imaginary part of the vector nonflip amplitude ( $\text{Im}F_0^{(-)}$ ) changes sign near  $t = -0.2$  and, in fact, is not far from the DAM form  $\sim J_0(R\sqrt{-t})$ . Again, this appears to be a well-established feature of vector exchange.<sup>3-8</sup> Notice that, in general, our  $KN$  CEX nonflip amplitudes are significantly smaller than the flip amplitudes, as conjectured in several phenomenological treatments.<sup>19</sup>

(v) The imaginary part of the tensor nonflip amplitude ( $\text{Im}F_0^{(+)}$ ) has a zero near  $t = -0.2$ , but also a second zero at  $t = -0.4$ ; certainly, among all imaginary parts it shows the largest deviation from the DAM form. Qualitatively similar are the conclusions of many analyses involving  $f_0$ ,<sup>26,5</sup>  $K^{**}$ ,<sup>6-8</sup> as well as  $A_2$ .<sup>27</sup> A partial deviation from the DAM form should, probably, be considered as a definite feature of  $\text{Im}F_0$  (tensor) in all hadronic reactions. As a result, in the present analysis  $\text{Im}F_0^{(\pm)}$  are approximately EXD at small ( $t$ ) ( $\text{Im}F_0^{(+)} \approx -\text{Im}F_0^{(-)}$ ,  $|t| \leq 0.3$ ), but not at larger  $|t|$ . In hypercharge-exchange reactions exchange degeneracy for  $\text{Im}F_0^{(\pm)}$  is violated even more.<sup>6-8</sup>

(vi) The real part of the vector nonflip amplitude ( $\text{Re}F_0^{(-)}$ ) deviates from the DAM form, and is not simply related to  $\text{Im}F_0^{(-)}$ . These two conclusions appear now well established; in fact,

most analyses involving vector exchange<sup>3-7</sup> give a shape much the same as that of our Fig. 5.

(vii) Finally, the real part of the tensor nonflip amplitude ( $\text{Re}F_0^{(\pm)}$ ) bears no simple relation to  $\text{Im}F_0^{(\pm)}$ , at least for  $|t| \geq 0.2$ . In the present analysis (Fig. 5) it changes sign at  $t \approx -0.2$ . Other analyses involving  $A_2$ ,  $f_0$ , or  $K^{**}$  (Refs. 4-8) show also  $\text{Re}F_0^{(\pm)}$  changing sign, but, in general, at larger  $|t|$ . It is likely that  $\text{Re}F_0^{(\pm)} = 0$  somewhere near  $t \approx -0.4$  is a common feature of all tensor exchanges in hadron reactions.

Once  $a^{(\pm)}(t)$  and  $b^{(\pm)}(t)$  have been determined, we can use the formalism of Sec. II to predict differential cross sections and polarizations for both  $K^-p \rightarrow \bar{K}^0n$  and  $K^+n \rightarrow K^0p$  at several energies ( $\nu > N$ ). Our predicted  $d\sigma/dt(K^-p \rightarrow \bar{K}^0n)$  at 5, 7.1, and 9.5 GeV are shown in Fig. 3; and our predicted  $d\sigma/dt(K^+n \rightarrow K^0p)$  at 5.5 GeV is shown in Fig. 4. Agreement with experiment is satisfactory. Figure 2 (broken line) shows our predicted polarization for  $K^+n \rightarrow K^0p$  at 8 GeV; the characteristic feature is very small values at  $|t| \leq 0.3$ , but large positive values at  $t \approx -0.6$  [roughly symmetric to  $P(K^-p \rightarrow \bar{K}^0n)$ ].

#### IV. COMPARISON WITH FESR AND WITH RECENT ANALYSES

The equations that determine  $a^{(\pm)}(t)$  and  $b^{(\pm)}(t)$  in terms of  $P(K^-p \rightarrow \bar{K}^0n)$ ,  $d\sigma/dt(K^-p \rightarrow \bar{K}^0n)$ , and  $d\sigma/dt(K^+n \rightarrow K^0p)$  at each value of  $t$  are nonlinear; thus there are more than one solution (here two, in general). We can discriminate between these solutions on the basis of FESR. Figure 6 shows the comparison of the selected solution with the lowest-moment FESR of Eqs. (2.17)-(2.20). The integrals of FESR have been calculated with the same low-energy information used for the dispersion integrals (resonances, etc. of Table I). In general for  $|t| \leq 0.4$  the comparison is satisfactory; also, with the exception of  $B^{(\pm)}$ , the FESR support the zero structure of our amplitudes.<sup>28</sup> Solutions other than the selected one are in marked contrast with FESR.

After completion of this work we received two reports<sup>29,30</sup> with analyses of  $KN$  CEX, and we now compare our results with them.

Reference 29 uses experimental data on  $\pi^-p \rightarrow \eta n$  and  $K^-p \rightarrow \bar{K}^0n$ , together with SU(3) symmetry and the assumption that the phase of the helicity-flip amplitude for vector exchange is Regge-pole-dominated, to perform an amplitude analysis of the tensor exchange. It can be said that, qualitatively, the conclusions of this work are in complete agreement with ours. Notice in particular their deduction of exchange degeneracy for  $\text{Im}F_1^{(\pm)}$  (used as an assumption in our work), and their conclusions

that  $F_1^{(+)}$  is consistent with Regge-pole dominance [Sec. III, point (iii)] and that  $\text{Im}F_0^{(+)}$  has two nearby zeros [point (vii)]. Our  $\text{Re}F_0^{(+)}$  is also within their error bars. Reference 26 also predicts the polarization for  $K^+n \rightarrow K^0p$  in qualitative agreement with ours.

Reference 30 is an application of KN FESR. The integrals of the left-hand side are calculated via phase-shift solutions (including a very recent one for  $I=0$  KN scattering) extending up to  $p_{\text{lab}} = 1.5$  GeV; then the right-hand side is used to obtain information on the  $t$  structure of the imaginary and real parts (the latter via continuous-moment sum-rule methods). Generally, their FESR results are in qualitative agreement with ours (in particular for  $\text{Im}F_1^{(-)}$  and  $\text{Im}F_0^{(-)}$ ); also their  $\text{Re}F_1^{(-)}$  agrees with ours. However, the details of the  $t$  structure of their  $A_2$  exchange amplitudes differ (e.g., their  $\text{Im}F_1^{(+)}$  and  $\text{Im}F_0^{(+)}$  violate DAM completely). It is possible that KN FESR, although very useful in providing qualitative tests (like selecting between various solutions) do not accurately reflect the  $t$  structure of all the high-energy ( $\geq 5$  GeV) amplitudes.<sup>12</sup>

#### ACKNOWLEDGMENT

One of us (A.P.C.) would like to thank Dr. H. Gordon, Dr. Kwan-Wu Lai, and Dr. N. P. Samios

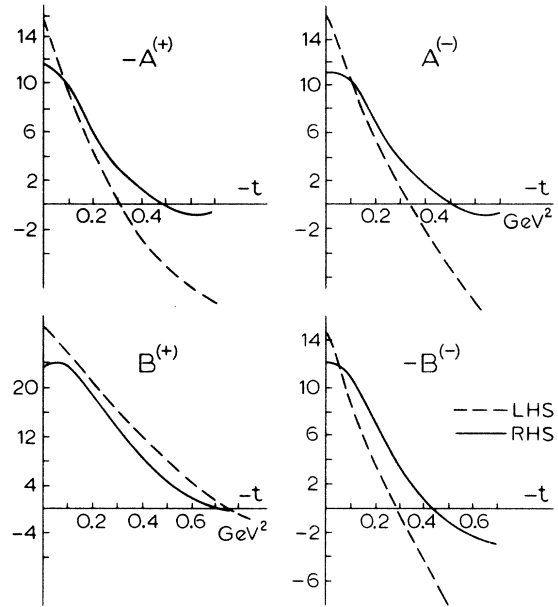


FIG. 6. Test of our solution against the lowest-moment FESR. LHS and RHS refer to the left- and right-hand side of Eqs. (2.17)–(2.20).

for a number of discussions and for the hospitality extended to him at Brookhaven during the summer of 1973.

\*Research supported by Physics Department, State University College of Arts and Science, Plattsburgh, New York 12901.

†Work also supported by the National Research Council of Canada.

<sup>1</sup>H. Harari, Phys. Rev. Lett. **26**, 1400 (1971); Ann. Phys. (N.Y.) **63**, 432 (1971).

<sup>2</sup>F. Halzen and C. Michael, Phys. Lett. **36B**, 367 (1971).

<sup>3</sup>R. L. Kelly, Phys. Lett. **39B**, 635 (1972).

<sup>4</sup>J. S. Loos and J. A. Matthews, Phys. Rev. D **6**, 2463 (1972).

<sup>5</sup>E. N. Argyres, A. P. Contogouris, and M. Svec, Phys. Rev. D **8**, 184 (1973); Ann. Phys. (N.Y.) (to be published).

<sup>6</sup>V. D. Barger, A. C. Irving, and A. D. Martin, Nuovo Cimento **16A**, 573 (1973); A. D. Martin, in *Two-Body Collisions*, Proceedings of the Seventh Rencontre de Moriond, Meribel-les-Allues, edited by J. Tran Thanh Van (CNRS, Paris, 1973).

<sup>7</sup>C. B. Chiu and E. Ugaz, Phys. Lett. **43B**, 327 (1973).

<sup>8</sup>E. N. Argyres, A. P. Contogouris, and J. P. Holden, Phys. Rev. D **9**, 1340 (1974).

<sup>9</sup>W. Beusch *et al.*, Phys. Lett. **46B**, 744 (1973).

<sup>10</sup>M. Coirier, J. Guillaume, Y. Leroyer, and Ph. Salin, Nucl. Phys. **B44**, 157 (1972).

<sup>11</sup>G. Ghandour and R. G. Moorhouse, Phys. Rev. D **6**, 856 (1972).

<sup>12</sup>E. N. Argyres, A. P. Contogouris, J. P. Holden, and M. Svec, Phys. Rev. D **8**, 2068 (1973).

<sup>13</sup>M. Hontebeyrie, J. Procureur, and Ph. Salin, Nucl. Phys. **B55**, 83 (1973).

<sup>14</sup>T. Barbeur and R. G. Moorhouse, CERN Report No. Th. 1712, 1973 (unpublished).

<sup>15</sup>Ph. Salin, rapporteur's talk at the International Symposium on Electron and Photon Interactions at High Energies, Bonn, 1973 [CERN Report No. Th. 1744 (unpublished)].

<sup>16</sup>R. D. Field and J. D. Jackson, Phys. Rev. D **4**, 693 (1971).

<sup>17</sup>P. T. Matthews and A. Salam, Phys. Rev. **110**, 569 (1958); B. R. Martin, in *Springer Tracts in Modern Physics*, edited by G. Höhler (Springer, New York, 1970), Vol. 55.

<sup>18</sup>L. Dick, in *Proceedings of the Second International Conference on Polarized Targets*, edited by G. Shapiro (Univ. of California Press, Berkeley, Calif., 1971).

<sup>19</sup>V. D. Barger and D. Cline, *Phenomenological Theories of High Energy Scattering* (Benjamin, New York, 1968); K.-W. Lai and J. Louie, Nucl. Phys. **B19**, 205 (1970).

<sup>20</sup>G. V. Dass and C. Michael, Phys. Rev. **175**, 1774 (1968).

<sup>21</sup>Particle Data Group, Rev. Mod. Phys. **45**, S1 (1973).

<sup>22</sup>N. P. Samios, M. Goldberg, and B. T. Meadows, BNL Report No. BNL 17851, 1973 (unpublished).

- <sup>23</sup>E. Pietarinen and C. P. Knudsen, Nucl. Phys. **B57**, 637 (1973).
- <sup>24</sup>J. K. Kim, Phys. Rev. Lett. **19**, 1074 (1967).
- <sup>25</sup>As a test, we have calculated the integrals along  $\bar{\nu} \leq \nu \leq \nu_0$  of (2.15) and (2.16) using the  $K$ -matrix formalism and the results of Ref. 24. At  $t \approx -0.2$  the results are very close to those obtained by resonance saturation. At  $t \approx -0.5$  there is some difference.
- <sup>26</sup>V. Barger, K. Geer and F. Halzen, Nucl. Phys. **B49**, 302 (1972).
- <sup>27</sup>J. P. Harnad, Ph.D. thesis, Oxford University, 1973 (unpublished).
- <sup>28</sup>The approximate relations (3.4) and (3.5) can be understood by the fact that the FESR for  $A^{(k)}$  are well satisfied for most  $t$ . This point is discussed in Ref. 12 and in the second paper of Ref. 5.
- <sup>29</sup>G. Girardi, C. Godreche, and H. Navelet, Nucl. Phys. **B76**, 541 (1974).
- <sup>30</sup>F. Elvekjaer and B. R. Martin, Nucl. Phys. **B75**, 388 (1974).
- <sup>31</sup>P. Astbury *et al.*, Phys. Lett. **23**, 2396 (1966).
- <sup>32</sup>A. Firestone *et al.*, Phys. Rev. Lett. **25**, 958 (1970).
- <sup>33</sup>D. Cline *et al.*, Nucl. Phys. **B22**, 247 (1970).

PHYSICAL REVIEW D

VOLUME 10, NUMBER 7

1 OCTOBER 1974

## Global description of $0^{-\frac{1}{2}+} \rightarrow 0^{-\frac{1}{2}+}$ reactions utilizing the bare Pomeron\*

N. F. Bali

*Physics Department, University of Washington, Seattle, Washington 98195*

Jan W. Dash

*High Energy Physics Division, Argonne National Laboratory, Argonne, Illinois 60439*

(Received 4 March 1974)

It is shown that the combination of a "bare Pomeron" with intercept  $\hat{\alpha}_P(0) = 0.85$  in conjunction with a reasonable set of secondary Regge trajectories and a canonical absorption prescription is capable of providing a good global fit to practically all  $0^{-\frac{1}{2}+} \rightarrow 0^{-\frac{1}{2}+}$  meson-nucleon scattering data up to lab momenta of 30 GeV/c. The bare Pomeron with intercept lower than 1 has a large real part which greatly facilitates the description of the data. At higher energies, "renormalization" effects can be expected to be important as inelastic diffraction events, and these lead to a renormalized Pomeron intercept very close to or equal to one. The value  $\hat{\alpha}_P(0) = 0.85$  used throughout this intermediate-energy fit is in agreement with current inclusive triple-Regge data and maximum-rapidity-gap distributions. It is also in agreement with certain strong-coupling ABFST (Amati-Bertocchi-Fubini-Stanghellini-Tonin) multiperipheral model calculations. For secondary effects, we have used a family of vector Regge trajectories ( $\rho, \omega, K^*$ ) with a degenerate intercept of about 0.45, and tensor trajectories ( $A_2, K^{**}$ ) with an intercept of about 0.25. A second vacuum pole emerges with intercept close to 0. The  $P'$  ( $f$ ) trajectory, not included here, can perhaps be expected to appear in conjunction with the renormalization of the Pomeron. Although no wrong-signature nonsense zeros are included in the parametrization, the  $\rho$ - $A_2$  and  $K^*$ - $K^{**}$  pole couplings are nevertheless very nearly exchange degenerate. SU(3) is used to relate most of the other couplings. The (pole + cut) helicity-flip  $\rho$ - $A_2$  and  $K^*$ - $K^{**}$  amplitudes also show considerable exchange-degenerate characteristics. We have used a standard absorption prescription to calculate the second-order bare Pomeron ( $\hat{P}$ )  $\otimes$  Reggeon cuts and  $\hat{P} \otimes \hat{P}$  cuts. An unusual result emerges—the "enhancement"  $\lambda_i$  factors for all cuts are less than one. This indicates the presence of higher-order cuts which thus dominate over inelastic intermediate-state production in this approach. The data used in this fit are a representative selection of  $0^{-\frac{1}{2}+} \rightarrow 0^{-\frac{1}{2}+}$  data (including  $\pi N$  amplitude analysis, hypercharge-exchange differential cross sections and polarizations;  $\pi^+ p$  and  $K^+ p$  total and differential cross sections, polarizations, and  $t = 0$  real-to-imaginary ratios; and  $\pi N$  and  $KN$  charge-exchange differential cross sections and polarizations) up to  $p_{\text{lab}} = 30$  GeV/c and  $|t| = 1.5$  (GeV/c)<sup>2</sup>.

### I. INTRODUCTION

A universal feature of all phenomenological Regge descriptions of two-body scattering data of the last ten years has been the use of a vacuum pole trajectory with intercept of (or very close to) 1.0, and a finite slope. This particular choice

has been traditionally suggested by the near constancy of the total and elastic cross sections and the behavior of the real-to-imaginary ratios of the forward elastic amplitudes. Thus, a simple Pomeron pole with intercept at 1, together with a restricted set of leading secondary trajectories and supplemented by an absorption prescription